ELSEVIER

Model free-kinetics applied to CTMA+ removal of AlMCM-41 molecular sieves

Antonio S. Araujo*, Valter J. Fernandes, Jr., Marcelo J.B. Souza,
Antonio O.S. Silva, Joana M.F.B. Aquino

Department of Chemistry, Federal University of Rio Grande do Norte, CP1662, 59078-970, Natal, RN, Brazil

Abstract

AlMCM-41 molecular sieves were synthesized starting from a hydrogel with the following molar composition—4.58 SiO_2:0.0485 Na_2O:1 CTMABr:0.038 Al_2O_3:200 H_2O. Cethyltrimethylammonium bromide (CTMABr) was used as structure template. The obtained materials were characterized by XRD, FT-IR and TG/DTG. The model-free kinetic algorithms were applied in order to determinate conversion, isoconversion and apparent activation energy to decomposition of the CTMA+ species from the AlMCM-41 materials.
© 2003 Elsevier B.V. All rights reserved.

1. Introduction

The MCM-41 is the main component of the M41S family, discovery by Mobil scientists [1,2]. The hexagonal mesoporous systems with high surface area open possibilities of generating the surface acidity necessary to catalyze organic reactions of the petroleum industry. The formation of the AlMCM-41 phase occurs according to the liquid crystal template (LCT) mechanism, in which tetrahedral SiO_4 and AlO_4 species react with the surfactant template under hydrothermal conditions [3–5]. A typical preparation of the AlMCM-41 needs basically a solvent, a template (surfactant molecule), a silica source and an aluminum source. The influence of aluminum source in the final quality of AlMCM-41 material has been studied in different papers [6–8]. Variables like pH, temperature, time, gel composition and nature of the precursors materials have great importance in the production of pure MCM-41 hexagonal phase.

In order to be used as adsorbents and in catalytic applications the MCM-41 materials need to pass for a process for removal of the template molecules in the pores. Some works studying the removal of those template molecules were published, of which the more mentioned are extraction by solvents, supercritical fluid extraction and calcination [9–11]. In most of the cases the authors give significant importance to the calcination for showing more efficient and to guarantee the complete removal of CTMABr (Fig. 1). The variables in a typical calcination process are time, temperature, heating rate, catalyst mass and calcination atmosphere. High temperatures favor a rapid cracking and elimination of the template species; however, it can destroy the ordered silica structure. The determination of the best calcination conditions like this is of fundamental importance in obtaining an exempt final material of organic template species with good preservation of the ordered silica structure. In this work, thermogravimetry is used for studying the kinetic parameters of CTMABr removal employing integral TG curves and a model-free kinetic method [12–14] to calculate the activation energy, the conversion rates and isoconversion parameters to evaluate the stage of decomposition of removal template species as function of temperature and time under dynamic flow conditions.

2. Experimental

The AlMCM-41 material was synthesized starting from silica gel (Merck), sodium silicate solution containing 63% SiO_2 and 18% Na_2O (Hiedel de Haen), cethyltrimethylammonium bromide (CTMABr, vetec) and distilled water.

* Corresponding author. Tel.: +55-84-2119241; fax: +55-84-2119241.
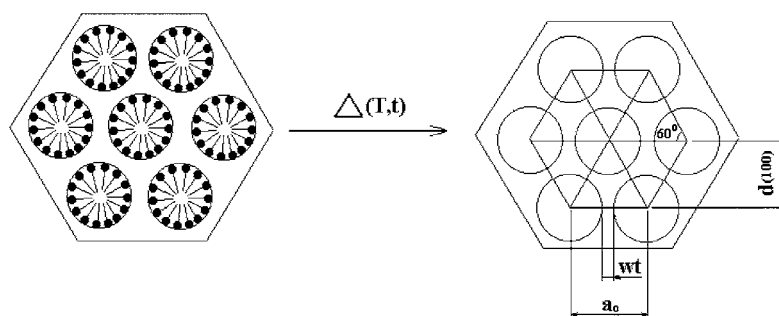*E-mail address:* asa-ufrn@usa.net (A.S. Araujo).

Fig. 1. Schematic representation of the mesoporous array of the MCM-41 before and after the calcination. (●) Surfactant molecule; T, temperature; t, time; wt, silica wall thickness; $d_{(100)}$, interplanar distance in the $(1\,0\,0)$ plane and a_0, mesoporous parameter [2].

Aluminum sources were used pseudobohemite (Vista). For the pH adjustment, 30% acetic acid in ethanol solution was used. The chemicals were mixed in order to obtain a gel with the following molar composition—4.58 SiO_2:0.0485 Na_2O:1 CTMABr:0.038 Al_2O_3:200 H_2O. The procedure used to obtain 1.3 g of calcined AlMCM-41 was (i) 0.856 g of silica, 0.783 g of sodium silicate and 5.0 g of distilled water were placed into a 50 ml Teflon Becker and stirred at 60 °C for 2 h; (ii) 0.026 g of pseudobohemite was placed in 3.0 g of distilled water and stirred at 60 °C for 1 h. The solution obtained in (ii) was added to the solution obtained in (i) and stirred at 60 °C for 30 min. A solution (iii) prepared from 1.74 g of cethyltrimethylammonim bromide and 8.63 g of distilled water was added to the (i) + (ii) mixture and aged for 1 h at room temperature. The hydrogel was placed into 45 ml teflon-lined autoclave and heated at 100 °C for 4 days. The obtained material was filtered, washed and dried at 100 °C in a stove for 2 h.

XRD measurements were carried out in Shimadzu equipment using Cu Kα radiation in 2θ angle of 1–$10°$ with step of $0.01°$. FT-IR curves were obtained in a BOMEM equipment model MB100. TG analysis was carried out in Mettler equipment, TGA/SDTA851 model, using nitrogen as gas carrier flowing at 25 ml min^{-1}. The samples as synthesized were heated from room temperature up to 900 °C, at a heating rate of 5, 10 and 20 °C min^{-1}. Vyazovkin and co-workers' model-free kinetics was used to evaluate the kinetic parameters of surfactant decomposition of the AlMCM-41 material as apparent activation energy, conversion rates and surfactant degradation time as function of temperature [12–14]. So were determined the optimal conditions of calcination to remove CTMA+ species from the mesoporous system of the AlMCM-41 samples.

3. Results and discussion

In several processes, the determination of a specific chemical reaction rate depends on conversion (α), temperature (T) and time (t). The reaction rate represented as a function of conversion $f(\alpha)$ is different for each process and must be determined experimentally. For simple reactions, the eval-

uation of $f(\alpha)$ with the nth order is possible. For complex reactions the function of (α) is complicated and generally unknown; in this cases the nth order algorithm causes unreasonable kinetic data. With the model-free kinetics, more accurate evaluations of complex reactions can be performed, as a trustworthy way of obtaining reliable and consistent kinetic information about the overall process [12]. Vyazovkin et al. developed an integral kinetic method where no model has to be selected [13,14] (model free-kinetics), which allows to evaluate both simple and complex reactions using multiple heating rates. The theory is based on $(\partial\alpha/\partial T) = k\mathrm{e}^{-E/RT}f(\alpha)$ and that the activation energy $E(\alpha)$ is constant for a certain conversion. The rate of the chemical reactions depends of the conversion (α), temperature (T) and time (t). The analysis is based on the isoconversion principle, which states that of constant conversion, the reaction rate is only a function of the temperature. The basic equation of non-isothermal kinetics is as follows:

$$\frac{\mathrm{d}\alpha}{\mathrm{d}T} = \frac{k}{\beta} f(\alpha), \tag{1}$$

where k is the rate constant (s^{-1}) and β is the heating rate (°C s^{-1}). Replacing k with the Arrhenius equation $k = k_0\mathrm{e}^{-E/RT}$ and rearranging the equation gives

$$\frac{1}{f_\alpha} \mathrm{d}\alpha = \frac{k_\beta}{\beta} \mathrm{e}^{-E/RT} \mathrm{d}T \tag{2}$$

Integrating the Eq. (2), gives

$$\int_0^\alpha \frac{1}{f_\alpha} \mathrm{d}\alpha = g(\alpha) = \frac{k_\beta}{\beta} \int_{T_0}^T \mathrm{e}^{-E/RT} \mathrm{d}T \tag{3}$$

Since $E/2RT \gg 1$, the temperature integral can be approximated by

$$\int_{T_0}^T \mathrm{e}^{-E/RT} \mathrm{d}T \approx \frac{R}{E}T^2 \mathrm{e}^{-E/RT} \tag{4}$$

Substituting the temperature integral, rearranging and taking logarithm gives

$$\ln\frac{\beta}{T_\alpha^2} = \ln\left[\frac{Rk_0}{E_\alpha g(\alpha)}\right] - \frac{E_\alpha}{R}\frac{1}{T_\alpha} \tag{5}$$
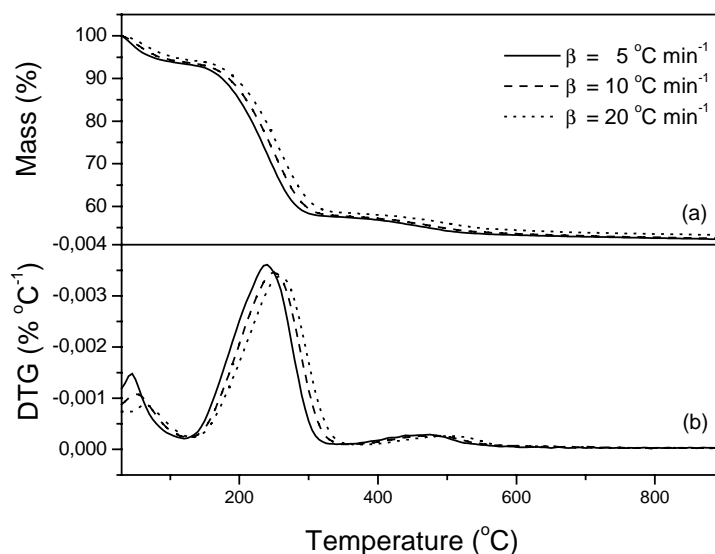
Fig. 2. (a) TG curves from uncalcined AlMCM-41 at different heating rates and (b) respective DTG curves.

In the typical experiment is necessary to obtain at least three different heating rates (β) and the respective conversion curves are evaluated from the measured TG curves. For each conversion (α), $\ln(\beta/T_\alpha^2)$ plotted versus $1/T_\alpha$, giving a straight line with slope $-E_\alpha/R$, therefore, the activation energy is obtained as function of the conversion. One of the great advantages of this model is the possibility to isolate the function $g(\alpha)$ in the linear coefficient. The determination of this function in complex process is very difficult to determine.

The kinetic data were obtained starting from TG measurements. Fig. 2 shows the TG curves at different heating rates of the AlMCM-41 sample in the uncalcined form and

its respective DTG curves. We can observe three typical mass losses [11]: (i) from 30 to 100 °C due to thermodesorption of physically adsorbed water, (ii) of 100–310 °C due to the primary surfactant decomposition and (iii) 310–600 °C due to residual surfactant decomposition. The (ii) and (iii) mass losses were attributed to the stages of CTMA+ decomposition and for them model-free algorithms were used to estimate the activation energy for each process. Fig. 3 presents the curves of the activation energy as function of conversion to each decomposition stage of CTMA+ from AlMCM-41 pores. The CTMA+ removal of the MCM-41 material was evaluated by thermogravimetry, at heating rates of 5, 10 and 20 °C min^{-1}. Fig. 4 shows
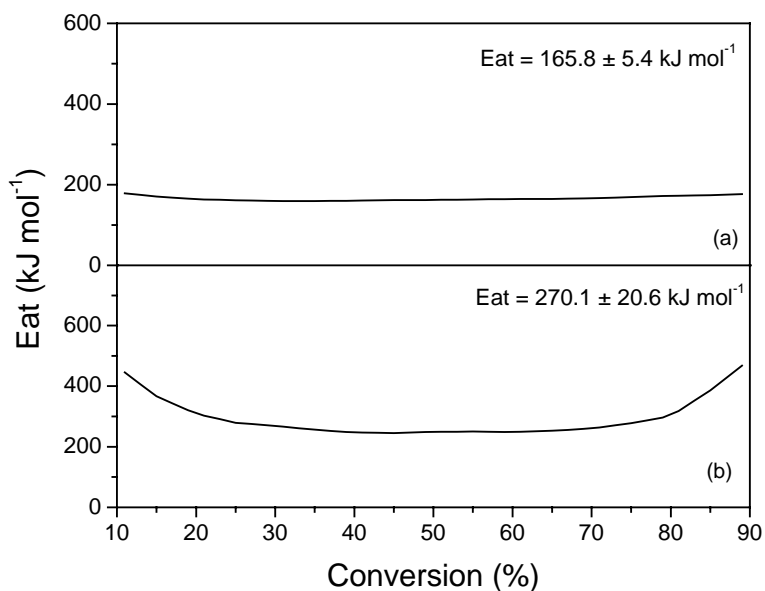

Fig. 3. Apparent activation energy to CTMA+ removal of the AlMCM-41 material (a) from 100 to 310 °C and (b) from 310 to 600 °C temperature range.
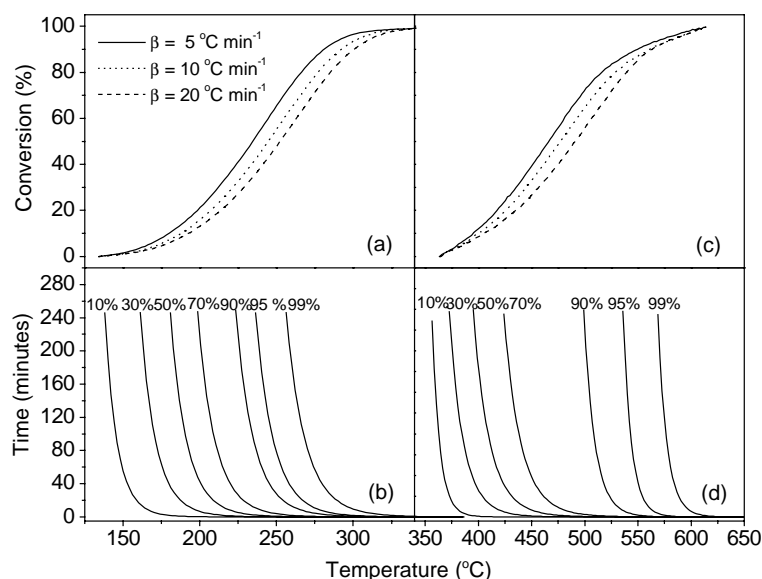
Fig. 4. Conversion and isoconversion curves of CTMA+ removal from AlMCM-41: (a and b) from 100 to 310 °C; and (c and d) from 310 to 600 °C, respectively.

the conversion and isoconversion curves at three different heating rates as function of the temperature obtained by the model-free kinetics.

The activation energy to removal of the CTMA+ species in the range of 100–310 °C and 310–600 °C were of ca. 165.8 and 270.1 kJ mol^{-1}, respectively. The obtained activation energy curve to each material can be used coupled with the model-free algorithms [12–14] to the estimation of conversion and isoconversion parameters at different stages of CTMABr decomposition. The Table 1 shows the values of the temperature removal of the CTMA+ as function of the conversion and time.

Table 1
Temperature to removal of CTMA+ of the AlMCM-41 at different events

Time (min)	10	30	50	70	90	95	99
Temperature range: 100–310 °C							
10	164.66	195.2	217.23	237.28	263.44	276.11	299.17
20	158.62	187.4	208.84	228.39	254.26	267.01	289.29
30	155.17	182.96	204.06	223.33	249.03	261.82	283.67
40	152.75	179.86	200.73	219.8	245.39	258.2	279.75
50	150.9	177.48	198.18	217.1	242.59	255.42	276.75
60	149.39	175.56	196.11	214.92	240.34	253.18	274.32
70	148.13	173.94	194.38	213.08	238.44	251.3	272.28
80	147.04	172.56	192.89	211.51	236.81	249.68	270.53
90	146.08	171.34	191.58	210.13	235.38	248.25	268.99
100	145.23	170.26	190.42	208.9	234.11	246.99	267.62
110	144.46	169.28	189.37	207.79	232.96	245.85	266.39
120	143.77	168.39	188.42	206.78	231.92	244.81	265.27
Temperature range: 310–600 °C							
10	379.74	416.87	446.87	477.35	533.15	561.63	596.47
20	374.5	406.82	435.07	465.09	525.54	555.94	590.3
30	371.48	401.08	428.35	458.11	521.16	552.65	586.73
40	369.35	397.07	423.66	453.23	518.09	550.32	584.21
50	367.71	393.99	420.06	449.49	515.71	548.53	582.27
60	366.38	391.49	417.15	446.46	513.79	547.08	580.69
70	365.25	389.39	414.71	443.92	512.16	545.85	579.36
80	364.28	387.59	412.61	441.74	510.76	544.79	578.21
90	363.43	386	410.76	439.82	509.53	543.86	577.2
100	362.67	384.59	409.12	438.12	508.43	543.02	576.3
110	361.98	383.32	407.64	436.58	507.45	542.27	575.48
120	361.35	382.16	406.3	435.18	506.54	541.58	574.74

After characterizing partially by TG, the next step to obtain the final AlMCM-41 phase is the calcination. In this step the sample will be submitted to effects of the temperature and time in a dynamic flow of gas (inert gas or oxidant atmosphere). The total removal of the template is mainly function of these variables. High temperatures favor a rapid template removal, but, by other side, excessive temperature can cause the destruction of the MCM-41 structure. The final samples of AlMCM-41 were obtained using four different treatments: (a) without calcination and (b), (c) and (d) with calcinations at 350, 500 and 650 °C, respectively. These temperatures were chosen based on the conversion and iso-conversion measurements. The conditions of the calcinations were heating rate of $10\,^{\circ}\text{C}\,\text{min}^{-1}$ in dynamic flow of N_2 at $25\,\text{ml}\,\text{min}^{-1}$. When the calcination temperatures were attained, the samples were kept by 120 min. Fig. 5 shows the XRD powder patterns for AlMCM-41 samples uncalcined and after calcination.

From the XRD measurements can be observed that the intensity of the pattern significantly increased with the increasing of the temperature of calcination, which is a known behavior related to the increase of contrast between the siliceous wall and the pore space after the surfactant has been removed [15]. In the case of sample obtained by the calcination method (d), a decrease in the peak intensity occurred probably due to excessive temperature (650 °C) that promoted total removal of the CTMABr molecules but with destruction of the ordered silica–alumina structure. The AlMCM-41 materials obtained using the methods (a), (b) and (c) showed characteristic peaks in the 2θ ranges of 1–10°, related to (1 0 0), (1 1 0), (2 1 0) Miller index, charac-
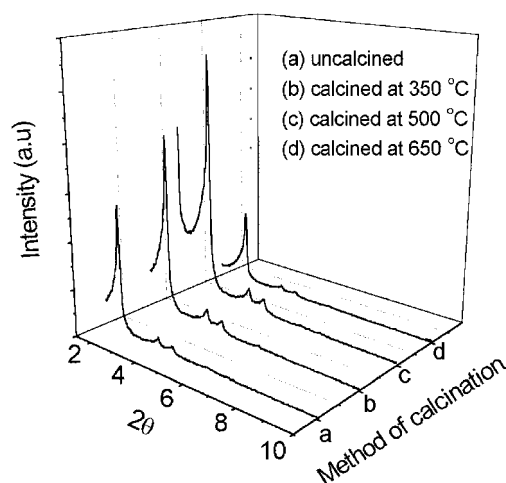

Fig. 5. XRD powder patterns of AlMCM-41 materials at different calcination conditions.

teristics of AlMCM-41 materials [1,2]. The sample calcined by the method (d) presented only the main peak related to the plane (1 0 0) due to the presence of a less ordered mesopore structure.

In order to evaluate the efficiency of the calcination process, FT-IR analysis were realized with the aim to observe elimination of the CTMA+ groups in the AlMCM-41 materials [16]. Fig. 6 shows the FT-IR analysis of the AlMCM-41 materials before and after the calcination. These materials were obtained by the methods (a), (b), (c) and (d) of calcination. Can be observed that the CTMA+ was fully removed in the samples obtained by the calcination
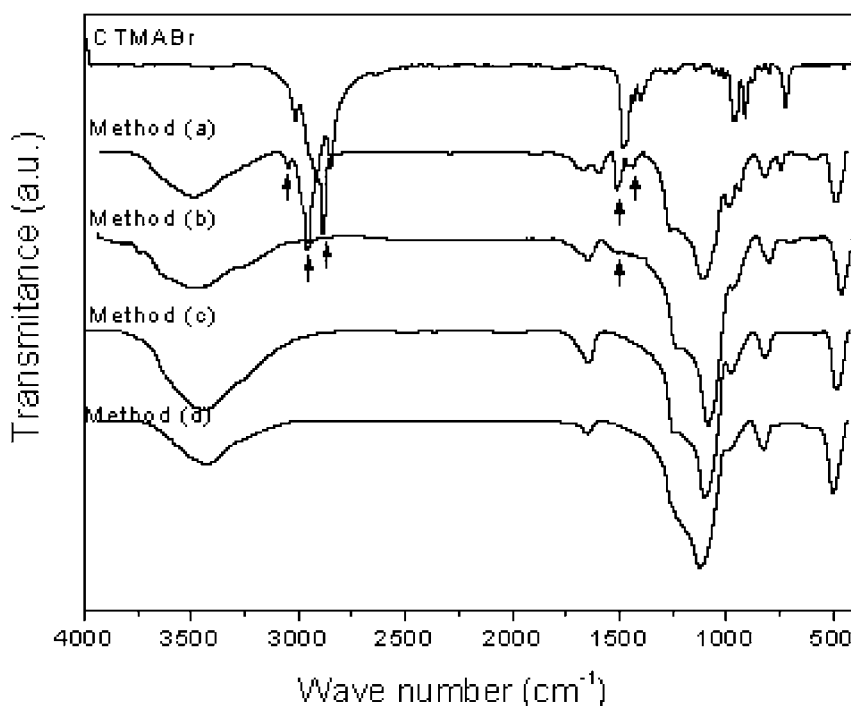

Fig. 6. FT-IR spectra of the CTMABr surfactant and AlMCM-41 materials prepared using different calcination methods.

methods (c) and (d), while in the sample obtained by the method (a) and (b) the removal was not satisfactory due to presence of very small amounts of CTMABr. This can be verified by the presence of the main functional groups of the CTMA+ species, by infrared. The spectra shows the following vibration bands: 3750–3250 cm^{-1} attributed to hydroxyl groups on mesoporous structure; 3000–2850 cm^{-1} as stretching of C–H bonds of CH$_2$ and CH$_3$ groups on CTMA+ species; 1700–1550 cm^{-1} as water physically adsorbed 1466–1460 cm^{-1} as asymmetric deformation of CH$_3$–R bond, 1475–1470 cm^{-1} as deformation of CH$_2$ bond; and 1490–1480 cm^{-1} as asymmetric deformation of head group methyl (CH$_3$–N+); 1260–1240 cm^{-1} as asymmetric Si–O stretching; 1200–1000 cm^{-1} as internal asymmetric T–O–T (T = Si, Al) stretching; 965–955 cm^{-1} as asymmetric CH$_3$–N+ stretching and 850–800 cm^{-1} due to symmetric T–O (T = Si, Al) stretching.

4. Conclusions

The present study show that in non-isothermal conditions, in which the sample was heated at three different and constant heating rates, the model-free kinetic analysis shows a good alternative to estimate the apparent activation energy to removal of CTMA+ species from AlMCM-41 materials. The apparent activation energy were ca. 165.8 and 270.1 kJ mol^{-1} in the range of 100–310 °C and 310–600 °C, respectively. XRD and FT-IR showed that model-free algorithms were satisfactory in the estimation of the conversion and isoconversion parameters obtaining high quality material under nitrogen atmosphere by calcination at 500 °C.

References

[1] X.S. Zhao, G.Q. Lu, G.J. Millar, Ind. Chem. Res. 35 (1996) 2075.
[2] J.S. Beck, J.C. Vartuli, W.J. Roth, M.E. Leonowicz, C.T. Kresge, K.D. Schmitt, C.T.W. Chu, D.H. Olson, E.W. Sheppard, S.B. Mc-Cullen, Y.B. Higgins, I.L. Schelenker, J. Am. Chem. Soc. 114 (1992) 10834.
[3] A.S. Araujo, C.D.R. Souza, M.J.B. Souza, V.J. Fernandes, L.A.M. Pontes, Stud. Surf. Sci. Catal. 141 (2002) 467.
[4] C.T. Kresge, M.E. Leonowicz, W.J. Roth, J.C. Vartuli, J.S. Beck, Nature 359 (1992) 710–712.
[5] A. Sayari, Stud. Surf. Sci. Catal. 102 (1996) 1.
[6] S.K. Badamali, A. Sakthivel, P. Selvam, Catal. Today 63 (2000) 291.
[7] M. Busio, J. Janchen, J.H.C. Van Hoff, Microporous Mesoporous Mater. 5 (1995) 211.
[8] Y. Cesteros, G.L. Haller, Microporous Mesoporous Mater. 43 (2001) 171.
[9] A.S. Araujo, M. Jaroniec, Thermochim. Acta 363 (2000) 175.
[10] R. Van Grieken, G. Galleja, G.D. Stucky, J.A. Melero, R.A. Garcia, J. Iglesias, Langmuir 19 (2003) 3966.
[11] S.A. Araujo, M. Ionashiro, V.J. Fernandes Jr., A.S. Araujo, J. Therm. Anal. Calorim. 64 (2001) 801.
[12] S. Vyazovkin, V. Goryachko, Thermochim. Acta 194 (1992) 221.
[13] S. Vyazovkin, A.I. Lesnikovich, Russ. J. Phys. Chem. 62 (1988) 2949.
[14] S. Vyazovkin, C.A. Wright, Thermochim. Acta 340 (1999) 53.
[15] B. Marler, U. Oberhagemann, S. Vortmann, H. Gies, Microporous Mesoporous Mater. 6 (1996) 375.